

e^{\pm} -CO and e^{\pm} -CO₂ total cross-section measurements

Ch. K. Kwan, Y.-F. Hsieh, W. E. Kauppila, S. J. Smith, T. S. Stein, and M. N. Uddin
Department of Physics and Astronomy, Wayne State University, Detroit, Michigan 48202

M. S. Dababneh

Department of Physics, Yarmouk University, Irbid, Jordan

(Received 20 October 1982)

As part of a continuing series of investigations, total scattering cross sections have been measured in the same apparatus for positrons and electrons colliding with CO and CO₂ using a beam-transmission technique. The projectile impact energies are in the range 1–500 eV for e^{\pm} -CO, 30–500 eV for e^+ -CO₂, and 100–500 eV for e^- -CO₂. An important aspect of our work is to compare the corresponding positron and electron total cross section (Q_T) curves for a given target gas. For both CO and CO₂ the electron Q_T values are generally larger than the positron results. For both gases at low energies there are relatively narrow shape resonances for electron scattering and noticeable increases in Q_T after the positronium-formation thresholds for positron scattering. At the highest energies investigated there are indications of a tendency toward merging of the positron and electron curves for each gas. A striking similarity is found between the present e^{\pm} -CO Q_T curves and the e^{\pm} -N₂ Q_T curves obtained by Hoffman *et al.* [Phys. Rev. A **25**, 1393 (1982)], in that the corresponding shapes and magnitudes are very nearly the same. Estimates of potential experimental errors, as well as the experimental discrimination against projectiles scattered at small forward angles, are made.

I. INTRODUCTION

Electron scattering by molecules, which plays an important role in a variety of collisional processes pertaining to gaseous lasers, planetary atmospheres, and energy generation, has been and continues to be the subject of many experimental and theoretical investigations. An approach that may help to provide a better understanding of electron-molecule scattering is to also study the scattering of positrons by the same molecules and to compare the corresponding results for positrons and electrons. The use of this approach to investigate and compare the total scattering of positrons and electrons by the inert gas atoms,^{1,2} and by H₂ and N₂,³ has revealed several interesting observations. An overall observation is that at low projectile energies (<20 eV) the measured total electron scattering cross sections by these gases are appreciably larger than the corresponding positron results, except when electron scattering experiences Ramsauer-Townsend effects (total cross-section minima) at very low energies. Meanwhile, at higher energies a general tendency toward merging of the positron and electron total cross-section curves is observed with an actual merging occurring for He and H₂ at energies above 200 eV. This gen-

eral behavior observed in the comparisons of positron and electron scattering by the above target gases can be explained qualitatively by the fact that the static interaction (attractive for electrons and repulsive for positrons) and polarization interaction (attractive for both projectiles) tend to add to each other for electron scattering and to cancel each other for positron scattering. At sufficiently high projectile energies only the static interaction will be significant, and a merging of the corresponding electron and positron total cross-section curves is expected. For further discussions of these positron and electron comparison measurements the reader is referred to two recent progress reports.^{4,5} The total cross-section measurements that we report here for positron and electron scattering by CO and CO₂ represent an extension of the earlier work of our group by Hoffman *et al.*³ for H₂ and N₂ at low and intermediate energies and for CO₂ at low energies.

II. THE EXPERIMENT

The experimental apparatus, procedure, and error analysis are the same as those used in prior total cross-section measurements reported from this laboratory^{1-3,6-9} and will only be briefly discussed here.

A Van de Graaff accelerator is used to generate an ¹¹C positron source from which a variable energy positron beam (energy width <0.1 eV) is extracted.¹⁰ For electron measurements, the positron source is replaced by a thermionic electron source (type B Philips cathode). Total scattering cross sections Q_T are deduced from the attenuation of the projectile beam by using the expression

$$I = I_0 e^{-nLQ_T}, \quad (1)$$

where I_0 is the detected beam current without gas in the scattering region, I is the detected beam current with gas of number density n present in the scattering region, and L is the beam path length through the scattering region.

The estimated errors in the present total cross-section measurements listed in Table I were obtained using the same procedure as outlined by Kauppila *et al.*¹ The "experimental error" estimates are obtained by taking the square root of the sum of the squares of each individual error component contributing to the potential errors in I , I_0 , n , and L , as well as the statistical error. The "maximum errors" represent the direct addition of each individual error component. The total errors for the positron and electron comparison measurements are smaller than those for the absolute total cross-section measurements for the same target gas because several of the individual error components would affect the positron and electron measurements equally. A standard check made in every data run is to measure total cross sections for several different target-gas densities to ensure that the results are independent of n , as shown in Fig. 1.

TABLE I. Estimated percentage errors in the present absolute and e^{\pm} comparison total cross-section measurements. Experimental errors are shown outside the parentheses while the maximum errors are enclosed by parentheses. Statistical errors in this table are typical values with the actual values for each data point listed in the Appendix. Estimated errors in this table do not include the potential errors associated with discrimination against small-angle scattering which are discussed separately.

	Projectile	
	e^+	e^-
Statistical	2(2)	1(1)
I, I_0	3(4)	2(2.5)
n	4(7)	4(7)
L	2(3)	1(2)
Total (absolute)	6(16)	5(12.5)
Total (e^{\pm} comparison)	4(8)	3(4.5)

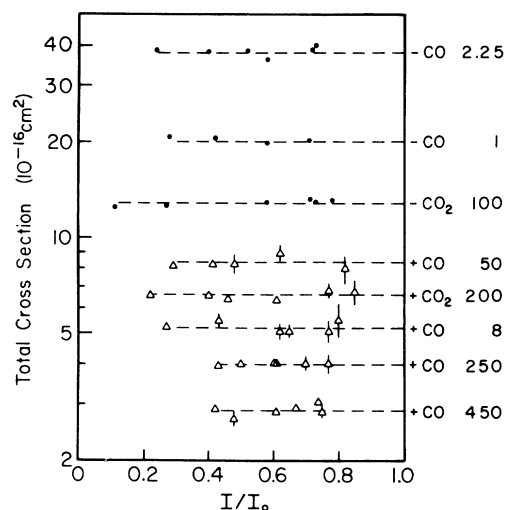


FIG. 1. Measured total cross sections as a function of attenuation ratios I/I_0 for various projectile-target combinations. A minus sign before the target symbol denotes electrons, positive sign denotes positrons. The projectile energy in eV follows the target symbol. The bars represent one standard deviation of the measured cross sections except when they are encompassed by the dots or triangles.

Another potential source of error, not included in Table I, relates to incomplete discrimination against projectiles that are scattered at small angles in the forward direction. As a result, the actual total cross sections may be larger than the measured values reported here. Two independent aspects of the present experiment that provide discrimination against small-angle scattering are the use of a retarding potential field after the scattering region and the use of a small exit aperture from the scattering region. Following the method of analysis of these effects by Kauppila *et al.*¹ we obtain the estimated discrimination angles for the present measurements as listed in Table II. It is to be noted that these estimated angles apply to elastic scattering and that the smaller of the two angles (R and A values) for each projectile-target-gas combination should represent an upper limit on the estimated angular discrimination for elastic scattering. In order to estimate the amount by which the measured total cross sections may be low, detailed information is required on the differential elastic-scattering cross sections and, depending on the projectile energies, inelastic scattering cross sections. It should be mentioned that in the present experiment there is complete discrimination against any inelastic scattering if the energy lost by the scattered projectile particle is more than a few tenths of an eV at low energies and a few eV at the higher energies due to the effect of the retarding

TABLE II. Estimated discrimination angles (in degrees) for elastic scattering deduced for the retarding potential procedure (R values) and for the effect due to the exit aperture size (A values). Columns are also labeled according to the target gases and projectile particles.

Energy (eV)	CO		CO ₂	
	e^+ R,A	e^- R,A	e^+ R,A	e^- R,A
5	31,20	11,6		
10	20,20	9,4		
30	10,22	5,4	17,16	5,4
50	11,17	4,4	22,18	4,4
100	10,14	4,4	15,16	6,4
300	8,8	6,5	8,15	7,4
500	9,8	5,5	16,7	5,4

element following the scattering region. As a result, the discrimination of this experiment against rotational and vibrational excitation processes may be incomplete (with estimated discrimination angles smaller than those given in Table II for elastic scattering), while discrimination against electronic excitation, ionization, and positronium formation should be complete.

III. RESULTS AND DISCUSSION

In the following discussions of the present results it should be realized that the experimental angular discriminations (see Sec. II) could affect both the reported absolute total cross-section values and the comparisons between the positron and electron measurements on the same gas. The present total cross-section measurements and associated statistical uncertainties are listed in the Appendix.

A. e^\pm -CO

Studies of electron scattering by carbon monoxide are not only interesting for their relevance to gaseous lasers and other applications involving ionized gases, such as magnetohydrodynamic (MHD) energy generation, but also because CO is isoelectronic with N₂. There have been many collision studies indicating that in many respects N₂ and CO scatter electrons similarly. Among these studies, Hake and Phelps¹¹ have recognized that the transport properties of electrons in CO resemble those for N₂, Schulz^{12,13} has discussed their somewhat similar behavior for electron-impact resonance formation and vibrational excitation, and Dubois and Rudd¹⁴ found that there are only minor differences in their respective differential elastic scattering cross sections at energies above 200 eV. These and other similarities between electron scattering by CO and

N₂ have also received recent theoretical attention¹⁵⁻¹⁸ (also see Ref. 15 for additional references). Comparisons such as these between CO and N₂, however, are also influenced by their basic differences, such as CO being a heteronuclear, nonsymmetric molecule having a weak permanent dipole moment.

The present total cross-section measurements for low-energy e^- -CO scattering are shown in Fig. 2 along with the results of prior experiments¹⁹⁻²² and a total cross-section (elastic scattering plus rotational excitation from $j=0$) calculation by Chandra,²³ who combined a single-center pseudopotential method with a frame-transformation theory (and a renormalized dipole term in the static potential). The most striking feature of the Q_T curve is the ²Π shape resonance, which we observe to be centered in

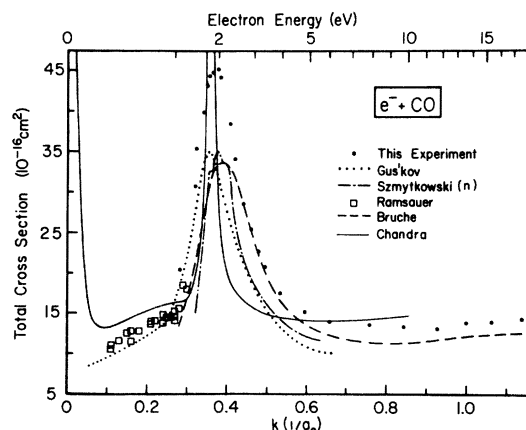


FIG. 2. Low-energy e^- -CO total cross sections. The present results are shown along with the measurements of Brüche (Ref. 19), Ramsauer and Kollath (Ref. 20), Szmytkowski and Zubek (Ref. 21), and Gus'kov *et al.* (Ref. 22), and the theoretical calculation of Chandra (Ref. 23). The n refers to normalized measurements.

the vicinity of 1.9 eV (with an uncertainty of a few tenths of an eV due to our energy calibration) with a maximum Q_T value of $45 \times 10^{-16} \text{ cm}^2$. In the calculation of Chandra²³ an adjustable parameter was used in the polarization potential in order to fix the resonance energy at about 1.75 eV. We made no special attempt to observe the weak oscillatory structure in the resonance peak that was seen by Szymkowski and Zubek²¹ because the energy width of our electron beam, less than 0.2 eV,¹⁰ is considerably larger than the energy resolution (< 0.05 eV) of the electron spectrometer used by Szymkowski and Zubek. Ehrhardt *et al.*²⁴ have observed a somewhat similar resonance structure in their elastic differential cross-section measurements. A comparison of the absolute Q_T experimental results shows that the present e^- -CO measurements are, in general, larger than the prior measurements.^{19,21,22} It is of interest to point out that the Q_T values of Szymkowski and Zubek²¹ are normalized values with their normalization being traceable to the 2–20 eV Q_T measurements of Golden and Bandel²⁵ for argon, and that earlier e^- -Ar Q_T measurements by our group⁶ (with the same experimental system as used here) average 10–15% higher than the results of Golden and Bandel. Therefore the actual discrepancy between our results and Szymkowski and Zubek, where the largest discrepancy (15–20%) exists at the resonance peak, is not as large as Fig. 2 would indicate. Our results average about 30% higher than Gus'kov *et al.*,²² which is greater than the combined estimated errors of each separate experiment (a maximum of 12% for our measurements and 10% for Gus'kov *et al.*). A comparison of our results with Brüche,¹⁹ when allowing for the slightly different energy location of the $^2\Pi$ resonance, shows that our results are 10–15% higher at energies above the resonance and about 30% higher at the resonance. In all cases, the general shapes of the experimental Q_T results versus energy are very similar. The calculation of Chandra²³ yields a $^2\Pi$ resonance that is noticeably narrower than the experimental results and considerably larger at the maximum ($69 \times 10^{-16} \text{ cm}^2$ and off scale in Fig. 2). Lane¹⁵ has commented that it would be expected that the theoretical result of Chandra for this resonance would be broadened and reduced in magnitude if vibrational effects had been included in the calculation. For energies above the $^2\Pi$ resonance the present results are in quite good agreement with the results of Chandra, while at energies below the resonance the results of Ramsauer and Kollath²⁰ and Gus'kov *et al.*²² have a quite similar shape (though somewhat lower in magnitude) to the theory, except at the lowest energies (< 0.1 eV) where the theory indicates a rapidly increasing total cross section.

The present low-energy e^+ -CO Q_T measurements are shown in Fig. 3 where they are compared with the results of Coleman *et al.*²⁶ Our results are everywhere higher than Coleman *et al.* and show a noticeable increase after the positronium-formation threshold.

The present Q_T results extending up to intermediate energies for e^{\pm} -CO scattering are shown in Fig. 4. The prior e^+ -CO results of Coleman *et al.*²⁶ are much lower than the present results above 30 eV due to their inability to effectively discriminate against small-angle forward scattering (elastic and inelastic) with their original time-of-flight system at these higher energies.^{4,5} From Fig. 4 it is seen that the present electron results are everywhere larger than the corresponding energy positron results with there being a tendency of the two curves to approach each other at the higher energies. The present positron Q_T results exhibit a rather broad maximum in the vicinity of 20 eV, while the electron curve possesses a secondary maximum in the same energy region.

Estimates of the amount by which the present e^- -CO Q_T measurements may be low due to incomplete discrimination against small-angle forward elastic scattering can be made by using the angular discrimination data in Table II (where the smaller of the R and A values is used) along with the recent intermediate energy (40–800 eV) differential elastic-scattering cross-section calculations for e^- -CO by Jain,¹⁷ who used a two-potential approach. This estimated error in Q_T ranges from less than 3% at 50 eV (where the elastic cross section of Jain accounts for 74% of the present Q_T result) to 9% at 500 eV (where the elastic cross section is 64% of Q_T). It is to be noted that incomplete discrimination against small-angle inelastic scattering (i.e., rotational and vibrational excitation) could also affect the present

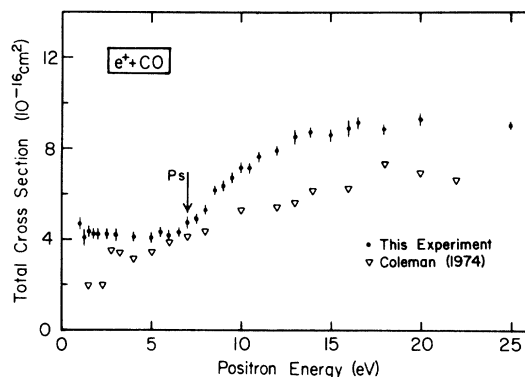


FIG. 3. Low-energy e^+ -CO total cross sections. The present results are shown along with the measurements of Coleman *et al.* (Ref. 26). The threshold for positronium formation (7.21 eV) is indicated by an arrow.

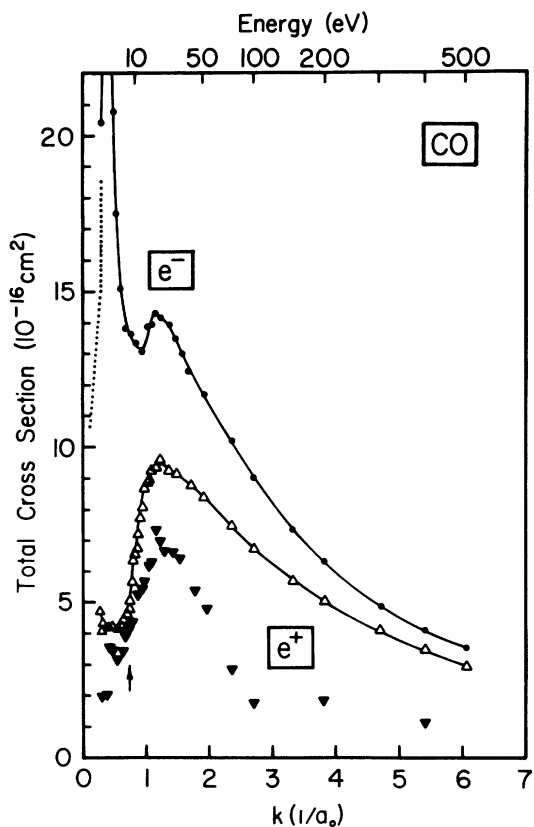


FIG. 4. Total e^{\pm} -CO scattering cross sections up to intermediate energies. The present measurements for electrons (\circ) and positrons (Δ) are shown with a solid line drawn through the respective points. The prior positron measurements of Coleman *et al.* (Ref. 26) are indicated by \blacktriangledown , while the dotted portion of the electron curve at low energies represents the measurements of Ramsauer and Kollath (Ref. 20). The positronium-formation threshold (7.21 eV) is indicated by the arrow.

Q_T measurements. We are unaware of the availability of sufficient differential cross-section information to make the latter estimates for inelastic e^- -CO scattering, as well as for e^+ -CO elastic and inelastic scattering.

Several particularly intriguing similarities can be seen by comparing the present e^{\pm} -CO Q_T curves with the corresponding e^{\pm} -N₂ measurements of Hoffman *et al.*³ (see Fig. 11 in Ref. 3). For electron total scattering from both CO and N₂ there is a low-energy shape resonance in the vicinity of 2 eV, $^2\Pi$ for CO, and $^2\Pi_g$ for N₂. In the vicinity of 20 eV both of these molecules exhibit a very similar secondary peak for electron scattering, which in the case of e^- -N₂ scattering may be attributed^{18,27,28} in part to a broad intermediate-energy shape resonance of σ_u symmetry in the vicinity of 25 eV. It is in-

teresting that Dehmer *et al.*²⁸ comment that many molecules may have intermediate-energy (~ 10 – 40 eV) shape resonances for electron scattering with verification having already been made for N₂, CO₂, OCS, CS₂, and SF₆. These resonances are in many cases too weak to be readily observed in elastic or total-scattering-cross-section measurements. Since CO is isoelectronic with N₂ and the shape of the present e^- -CO curve is very similar to the e^- -N₂ curve of Hoffman *et al.*,³ it seems reasonable that the 20-eV maximum in the e^- -CO Q_T curve may indicate the presence of an intermediate-energy shape resonance. This latter comment is consistent with the work of Truhlar *et al.*,²⁹ who found that vibrational excitation of both N₂ and CO by electron impact at 20 eV appears to be dominated by resonance scattering. The shapes of the Q_T curves for positron scattering from CO and N₂ are also remarkably similar to each other, both having an appreciable increase after the positronium-formation threshold and reaching a broad maximum in the vicinity of 20 eV for CO and 30 eV for N₂. Perhaps the most remarkable similarities between the present Q_T measurements for CO and the earlier measurements of Hoffman *et al.*³ for N₂ are that for energies above 50 eV the present e^- -CO results average only 2% larger than the corresponding e^- -N₂ results³ and the present e^+ -CO results average 3% larger than the e^+ -N₂ results.³ Just as the uncertainties for the e^{\pm} comparison Q_T measurements made in our experimental system are smaller than those for our absolute Q_T measurements, the comparisons of our e^+ -CO to e^+ -N₂ (Ref. 3) and e^- -CO to e^- -N₂ (Ref. 3) Q_T measurements also have smaller uncertainties associated with them. In addition, the comparisons of the e^- -CO results with the e^- -N₂ results should not be affected appreciably by angular discrimination effects because the calculations of Jain¹⁷ for e^- -CO and e^- -N₂ indicate that their respective differential elastic scattering cross sections are almost the same above 200 eV and very close to each other even at 40 eV. As a consequence, the shapes of the corresponding Q_T curves and the tendency toward merging of the respective e^{\pm} curves are nearly identical above 50 eV for CO and N₂. At projectile energies below 50 eV the Q_T values for e^{\pm} -CO scattering are also larger but close to the corresponding e^{\pm} -N₂ results.³ It seems particularly relevant that the integrated elastic cross sections obtained by Jain¹⁷ for e^- -CO and e^- -N₂ scattering are within 1% of each other above 200 eV, and the CO values are 8% larger at 40 eV. As mentioned earlier, our present electron Q_T results for CO (when compared to the results for N₂ from Ref. 3) range from 2% higher for energies greater than 100 eV to about 4% higher at 40 eV. Realizing that the calcu-

lation of Jain is less reliable at 40 eV than the higher energies, there is a remarkable consistency between the comparison of the present e^- -CO and prior³ e^- -N₂ Q_T measurements, and the comparison of the integrated elastic cross-section calculations for e^- -CO and e^- -N₂ of Jain. This consistency should be quite meaningful because the elastic cross sections of Jain account for 64% (at 500 eV) to 80% (at 40 eV) of the present Q_T results for CO and N₂, and also because the theoretical differential elastic cross sections for CO and N₂ are generally in very good agreement with each other and also with several prior experiments (see Figs. 4–10 in Ref. 17).

B. e^{\pm} -CO₂

As mentioned earlier, Hoffman *et al.*³ have recently reported low-energy e^{\pm} -CO₂ total cross-section measurements made in our laboratory. The low-energy positron and electron Q_T curves (refer to Figs. 12 and 13 of Ref. 3), in general, have a quite similar shape with the electron Q_T values being less than twice as large as the corresponding positron values. The notable differences in these respective curves are the shape resonance (occurring in Π_u symmetry) for electron scattering in the vicinity of 4 eV and the noticeable bump in the positron curve after the positronium-formation threshold at 7.0 eV.

The present Q_T results for intermediate-energy e^+ -CO₂ scattering are displayed in Fig. 5 where it can be seen that they merge into the measurements of Hoffman *et al.*³ and together indicate a broad cross-section maximum in the vicinity of 30–40 eV. The present results are appreciably higher than the measurements of Coleman *et al.*³⁰ which are known to be significantly low due to incomplete discrimina-

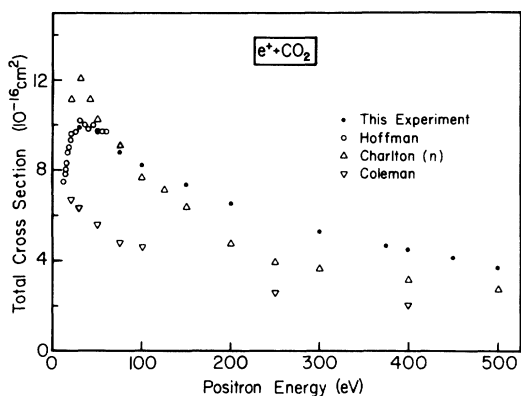


FIG. 5. Intermediate-energy e^+ -CO₂ total cross sections. The present results are shown along with the measurements of Coleman *et al.* (Ref. 30), Charlton *et al.* (Ref. 31) (where the n refers to normalized measurements), and Hoffman *et al.* (Ref. 3).

tion against small-angle scattering. A comparison of the present results with the normalized measurements of Charlton *et al.*,³¹ whose normalization constant was determined by Griffith *et al.*³² and traces back to the (30–100)-eV e^+ -He Q_T measurements of Coleman *et al.*,³³ is somewhat puzzling because Charlton *et al.* are consistently higher (up to 16%) than the present results for energies below 75 eV and up to 30% lower than our measurements above 75 eV. It seems unlikely that any single source of error in either experiment could explain the discrepancy unless the angular discrimination (i.e., the ability to discriminate against small-angle scattering) of Charlton *et al.* is better than the present work at energies below 75 eV and degenerates to a poorer angular discrimination (due to their time-of-flight approach) at the higher energies. Unfortunately, there is no differential scattering information available with which we could estimate the amount by which our e^+ -CO₂ Q_T measurements could be low as a result of our estimated angular discriminations given in Table II.

The present intermediate-energy e^- -CO₂ measurements are shown in Fig. 6 where they are com-

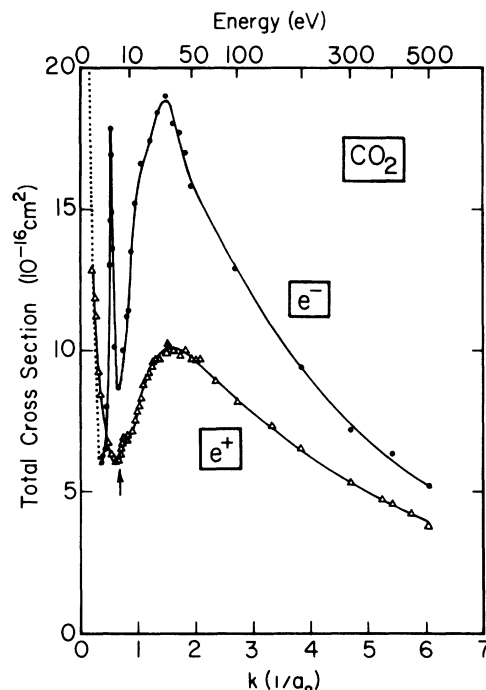


FIG. 6. A comparison of e^{\pm} -CO₂ total cross sections up to intermediate energies. The solid curves are drawn through a combination of the present measurements and those of Hoffman *et al.* (Ref. 3). The dotted curve at the lowest energies represents the electron measurements of Ferch *et al.* (Ref. 34). The arrow indicates the positronium-formation threshold energy at 6.97 eV.

TABLE III. Present total cross-section results with statistical uncertainties (in units of 10^{-16} cm²) for e^{\pm} -CO and e^{\pm} -CO₂ scattering.

E (eV)	Q_T (e^+ -CO)	E (eV)	Q_T (e^- -CO)
1.0	4.7 ±0.25	1.08	20.4 ±0.2
1.25	4.04±0.30	1.38	30.8 ±0.4
1.5	4.35±0.20	1.43	35.4 ±0.4
1.75	4.20±0.20	1.57	39.9 ±0.3
2.0	4.20±0.20	1.68	43.2 ±0.7
2.5	4.27±0.20	1.70	44.3 ±0.5
3.0	4.20±0.30	1.81	44.7 ±0.3
4.0	4.15±0.20	1.96	45.2 ±0.6
5.0	4.1 ±0.2	2.00	44.1 ±0.3
5.5	4.3 ±0.2	2.26	38.4 ±0.4
6.0	4.2 ±0.2	2.4	34.2 ±0.5
6.5	4.3 ±0.2	2.6	28.6 ±0.4
7.0	4.7 ±0.2	2.9	25.4 ±0.2
7.5	4.9 ±0.2	3.1	22.7 ±0.3
8.0	5.3 ±0.2	3.3	20.7 ±0.3
8.5	6.2 ±0.15	3.9	17.5 ±0.2
9.0	6.4 ±0.2	4.8	15.1 ±0.1
9.5	6.7 ±0.3	5.9	13.8 ±0.06
10.0	7.2 ±0.2	7.9	13.65±0.08
10.5	7.1 ±0.2	9.8	13.36±0.08
11.0	7.6 ±0.2	11.7	13.1 ±0.1
12.0	7.9 ±0.2	13.7	13.85±0.08
13.0	8.5 ±0.3	15.7	13.92±0.1
14.0	8.7 ±0.2	17.7	14.3 ±0.1
15.0	8.6 ±0.25	19.8	14.15±0.1
16.0	8.9 ±0.4	25.0	13.94±0.1
16.5	9.1 ±0.2	30.0	13.42±0.1
18.0	8.9 ±0.2	35.0	12.8 ±0.07
20.0	9.35±0.25	40.0	12.45±0.08
25.0	9.05±0.15	50.0	11.72±0.07
30.0	9.0 ±0.15	75.0	10.18±0.08
40.0	8.7 ±0.2	100.0	9.01±0.05
50.0	8.25±0.15	150.0	7.43±0.04
75.0	7.45±0.15	200.0	6.30±0.04
100.0	6.7 ±0.1	300.0	4.85±0.04
150.0	5.6 ±0.1	400.0	4.12±0.03
200.0	5.0 ±0.1	500.0	3.56±0.03
300.0	4.1 ±0.15		
400.0	3.47±0.05		
500.0	2.93±0.06		

E (eV)	Q_T (e^+ -CO ₂)	Q_T (e^- -CO ₂)
30	9.9 ±0.15	
50	9.6 ±0.2	
75	8.8 ±0.15	
100	8.2 ±0.1	12.9 ±0.1
150	7.3 ±0.1	
200	6.5 ±0.1	9.27±0.18
300	5.27±0.10	7.12±0.03
375	4.70±0.10	
400	4.55±0.10	6.26±0.08
450	4.16±0.08	
500	3.75±0.20	5.16±0.02

bined with the measurements of Hoffman *et al.*³ in order to establish a smooth Q_T curve, representing the electron results from our laboratory, which exhibits a maximum in the vicinity of 30 eV. To complete the e^- -CO₂ curve, the results of Ferch *et al.*³⁴ are displayed below 2 eV. The Q_T measurements of Brüche¹⁹ (not shown in Fig. 6) average from 10% to 20% lower than the present results in the region of the maximum, which is quite consistent with the corresponding comparisons for CO (see Fig. 2) and H₂ and N₂ (see Ref. 3). Shyn *et al.*³⁵ have deduced e^- -CO₂ elastic scattering cross sections for electron energies up to 90 eV from their differential cross-section measurements, and it is found that their $Q(\text{elastic})$ values average nearly 20% larger than our results between 10 and 40 eV, and they become lower for energies above 50 eV. There is somewhat of a discrepancy between these two sets of results since $Q(\text{elastic})$ should be $\leq Q_T$, but, the difference of 20% may be explained by the overlap of the quoted potential errors of these two experiments. In any case the $Q(\text{elastic})$ results of Shyn *et al.* seem to indicate that for energies below 50 eV Q_T may be composed primarily of elastic scattering. A calculation by Lynch *et al.*³⁶ (using the continuum multiple-scattering model) of $Q(\text{elastic})$ for energies up to 100 eV gives results that would account for about 70–80% of our Q_T results between 20 and 100 eV. The work of Lynch *et al.* also indicates the existence of some weak shape resonances in the energy range 10–40 eV. It is interesting that the earlier measurements of Hoffman *et al.* (see Fig. 13 of Ref. 3) may indicate an abnormal bump between 10 and 20 eV which may be related to an intermediate-energy shape resonance.

The comparison of the e^{\pm} -CO₂ curves in Fig. 6 shows that the electron results are everywhere larger than the positron results, except for projectile energies below 3 eV. With the exceptions of the low-energy shape resonance for electrons and the bump after the positronium-formation threshold for positrons, the shapes of the e^{\pm} curves are somewhat similar in that they both increase at the lowest energies and have a maximum in the vicinity of 30 eV, although the positron maximum is broader. At the

higher energies there seems to be a gradual tendency toward merging of the respective curves.

It is somewhat interesting to compare several features of the corresponding e^{\pm} -CO and e^{\pm} -CO₂ Q_T curves because these target molecules only differ by a single oxygen atom. As a result, however, CO₂ is symmetric and does not possess a permanent dipole moment, which is in contrast to the case for CO. Both molecules exhibit a low-energy shape resonance for electron scattering with the CO resonance being the more prominent one. The >10-eV maxima for the e^{\pm} curves occur at a higher energy for CO₂ (in the vicinity of 30 eV) than for CO (about 20 eV) with the electron maximum for each molecule appearing to be narrower than the maxima for positrons. For energies above 100 eV the e^- -CO₂ results average about 50% larger than the e^- -CO values, while the e^+ -CO₂ results average about 30% larger than for e^+ -CO. This tendency for the CO₂ measurements to be larger might be what one would expect since it possesses an extra atom.

In conclusion, we would like to point out that the present e^{\pm} Q_T measurements for CO and CO₂ are consistent with the earlier e^{\pm} Q_T comparison measurements for He, Ne, Ar, Kr, Xe, H₂, and N₂ from our group^{1–3} because in all cases the cross-section maxima (excluding low-energy shape resonances) for electron scattering are narrower than for positron scattering. This general observation could be related to the realization that the electron maxima for these target gases are primarily due to elastic scattering, while the positron maxima seem to be associated with inelastic processes.

ACKNOWLEDGMENTS

We gratefully acknowledge the helpful assistance of P. Felcyn, D. Jerius, and A. Sternad in various aspects of this project. This work was supported by the National Science Foundation under Grant No. PHY 80-07984.

APPENDIX

In Table III we present our e^{\pm} -CO and e^{\pm} -CO₂ total cross-section results.

¹W. E. Kauppila, T. S. Stein, J. H. Smart, M. S. Dababneh, Y. K. Ho, J. P. Downing, and V. Pol, *Phys. Rev. A* **24**, 725 (1981).

²M. S. Dababneh, Y.-F. Hsieh, W. E. Kauppila, V. Pol, and T. S. Stein, *Phys. Rev. A* **26**, 1252 (1982).

³K. R. Hoffman, M. S. Dababneh, Y.-F. Hsieh, W. E. Kauppila, V. Pol, J. H. Smart, and T. S. Stein, *Phys.*

Rev. A **25**, 1393 (1982).

⁴W. E. Kauppila and T. S. Stein, *Can. J. Phys.* **60**, 471 (1982).

⁵T. S. Stein and W. E. Kauppila, in *Physics of Electronic and Atomic Collisions*, edited by S. Datz (North-Holland, Amsterdam, 1982), pp. 311–329.

⁶W. E. Kauppila, T. S. Stein, and G. Jesion, *Phys. Rev.*

- Lett. **36**, 580 (1976).
- ⁷W. E. Kauppila, T. S. Stein, G. Jesion, M. S. Dababneh, and V. Pol, *Rev. Sci. Instrum.* **48**, 822 (1977).
- ⁸T. S. Stein, W. E. Kauppila, V. Pol, J. H. Smart, and G. Jesion, *Phys. Rev. A* **17**, 1600 (1978).
- ⁹M. S. Dababneh, W. E. Kauppila, J. P. Downing, F. Laperriere, V. Pol, J. H. Smart, and T. S. Stein, *Phys. Rev. A* **22**, 1872 (1980).
- ¹⁰T. S. Stein, W. E. Kauppila, and L. O. Roellig, *Rev. Sci. Instrum.* **45**, 951 (1974); *Phys. Lett.* **51A**, 327 (1975).
- ¹¹R. D. Hake, Jr. and A. V. Phelps, *Phys. Rev.* **158**, 70 (1967).
- ¹²G. J. Schulz, *Rev. Mod. Phys.* **45**, 423 (1973).
- ¹³G. J. Schulz, in *Principles of Laser Plasmas*, edited by George Bekefi (Wiley, New York, 1976), Chap. 2.
- ¹⁴R. D. Dubois and M. E. Rudd, *J. Phys. B* **9**, 2657 (1976).
- ¹⁵N. F. Lane, *Rev. Mod. Phys.* **52**, 29 (1980).
- ¹⁶K. Onda and D. G. Truhlar, *J. Chem. Phys.* **73**, 2688 (1980).
- ¹⁷A. Jain, *J. Phys. B* **15**, 1533 (1982).
- ¹⁸J. L. Dehmer and D. Dill, in *Electronic and Atomic Collisions*, edited by N. Oda and K. Takayanagi (North-Holland, Amsterdam, 1980), p. 195.
- ¹⁹E. Brüche, *Ann. Phys. (Leipzig)* **83**, 1065 (1927).
- ²⁰C. Ramsauer and R. Kollath, *Ann. Phys. (Leipzig)* **10**, 143 (1931).
- ²¹C. Szmytkowski and M. Zubek, *Chem. Phys. Lett.* **57**, 105 (1978).
- ²²Yu. K. Gus'kov, R. V. Savvov, and V. A. Slobodyan-yuk, *Fiz. Plazmy* **4**, 941 (1978) [*Sov. J. Plasma Phys.* **4**, 527 (1978)].
- ²³N. Chandra, *Phys. Rev. A* **16**, 80 (1977).
- ²⁴H. Ehrhardt, L. Langhans, F. Linder, and H. S. Taylor, *Phys. Rev.* **173**, 222 (1968).
- ²⁵D. E. Golden and H. W. Bandel, *Phys. Rev.* **149**, 58 (1966).
- ²⁶P. G. Coleman, T. C. Griffith, and G. R. Heyland, *Appl. Phys.* **4**, 89 (1974).
- ²⁷D. Dill, J. Welch, J. L. Dehmer, and J. Siegel, *Phys. Rev. Lett.* **43**, 1236 (1979).
- ²⁸J. L. Dehmer, J. Siegel, J. Welch, and D. Dill, *Phys. Rev. A* **21**, 101 (1980).
- ²⁹D. G. Truhlar, S. Trajmar, and W. Williams, *J. Chem. Phys.* **57**, 3250 (1972).
- ³⁰P. G. Coleman, T. C. Griffith, G. R. Heyland, and T. L. Killeen, *Atomic Physics 4* (Plenum, New York, 1975), p. 355.
- ³¹M. Charlton, T. C. Griffith, G. R. Heyland, and G. L. Wright, *J. Phys. B* **13**, L353 (1980).
- ³²T. C. Griffith, G. R. Heyland, K. S. Lines, and T. R. Twomey, *Appl. Phys.* **10**, 431 (1979).
- ³³P. G. Coleman, T. C. Griffith, G. R. Heyland, and T. R. Twomey, *Appl. Phys.* **11**, 321 (1976).
- ³⁴J. Ferch, C. Masche, and W. Raith, *J. Phys. B* **14**, L97 (1981).
- ³⁵T. W. Shyn, W. E. Sharp, and G. R. Carignan, *Phys. Rev. A* **17**, 1855 (1978).
- ³⁶M. G. Lynch, D. Dill, J. Siegel, and J. L. Dehmer, *J. Phys. Chem.* **71**, 4249 (1979).